Dalton Transactions

An international journal of inorganic chemistry

Accepted Manuscript

This article can be cited before page numbers have been issued, to do this please use: S. Grenda, H. Yairi, T. Fujimoto, O. Fabelo, I. Kibalin, N. Claiser, R. Maurice, A. Gukasov, L. Canadillas-Delgado, J. A. Rodriguez-Velamazan, J. Jacquot, R. Mitsuhashi, M. Mikuriya, M. Handa and D. Luneau, *Dalton Trans.*, 2026, DOI: 10.1039/D6DT00342G.

ROYAL SOCIETY OF CHEMISTRY

rsc.li/dalton

The Electron and Spin Distributions and Magnetic Anisotropy in Mixed-Valent Diruthenium(V) Tetracarboxylates from Crystallography and Theory

View Article Online
DOI: 10.1039/D6DT00342G

Sabrina Grenda*,[a], Haruki Yairi[b], Torao Fujimoto[b], Oscar Fabelo,[c] Iurii Kibalin,#[c] Nicolas Claiser,[e] Rémi Maurice,[f] Arsen Gukasov,[d] Laura Canadillas-Delgado,[c] José A. Rodriguez Velamazan,[c] Jean-François Jacquot,[g] Ryoji Mitsuhashi,#[h] Masahiro Mikuriya,[h] Makoto Handa*,[b] and Dominique Luneau*[a]

Author Affiliations

[a] Laboratoire des Multimatériaux et Interfaces (UMR CNRS 5615)
Université Claude Bernard Lyon 1
69100 Villeurbanne 69100
France
E-mail: dominique.luneau@univ-lyon1.fr

[b] Department of Chemistry
Graduate School of Natural Science and Technology
Shimane University
1060 Nishikawatsu
Matsue 690-8504
Japan

[c] Institut Laue-Langevin
71 avenue des Martyrs
38042 Grenoble Cedex 9
France

[d] Laboratoire Léon Brillouin (LLB),
CEA-CNRS (UMR CNRS 12)
CEA. Saclay
91191 Gif-sur-Yvette
France

[e] CRM2 (UMR CNRS 7036)
Université de Lorraine
BP70239
54506 Vandoeuvre-les-Nancy
France

[f] Univ Rennes, CNRS ISCR (Institut des Sciences Chimiques de Rennes) – UMR 6226
35000 Rennes
France

View Article Online
DOI: 10.1039/D6DT00342G

[g] CEA-Grenoble
38054 Grenoble
France

[h] School of Science and Technology
Kwansei Gakuin University
Sanda
669-1330
Japan

View Article Online
DOI: 10.1039/D6DT00342G

Abstract:

The determination of the electron and spin density distributions of the tetracarboxylato mixed-valent diruthenium(II,III) complex $(NBu_4)[Ru_2{}^{V}Br_2(O_2CC_3H_7)_4]$ was carried out using high-resolution X-ray diffraction and polarized neutron diffraction (PND) on single crystals. Experimental and theoretical spin distributions show that the spin density is predominantly localized on the ruthenium atoms with some delocalization onto bromide and carboxylate ligands. The charge-density analysis supports these findings, showing charge accumulation on the metal centres and typical donor–acceptor ligand–metal interactions. Experimental topological analysis of the Ru---Ru bond confirm an open-shell metal-metal interaction. The local magnetic anisotropy was explored through angle-resolved magnetic susceptibility measurements and PND. Magnetic data reveals significant magnetic anisotropy with an easy axis along the crystallographic *c* axis and the hard magnetization axis along the *b* crystallographic axis. Local magnetic susceptibility tensors derived from PND highlight pronounced planar magnetic anisotropy oriented along the equatorial Ru-O plane. The experimentally determined anisotropy parameters are in excellent agreement with ab initio calculations.

View Article Online
DOI: 10.1039/D6DT00342G

Introduction

The first mixed-valence tetracarboxylato diruthenium(II,III) compound $[Ru_2^V(O_2CCH_3)_4Cl]_n$ with a lantern-type structure of the tetra-*n*-butyratodiruthenium core, or paddlewheel structure as so-called today, was discovered six decades ago[1]. Analysis of the structural features from X-ray diffraction on single crystal showed the two ruthenium ions to be equivalent at a short Ru-Ru distance (2.28 Å) suggesting an average oxidation state of +2.5 for each ruthenium ion and the presence of a Ru-Ru bond[2]. At this time, this brought a corner-stone to the freshly identified quadruple and δ bonds by Cotton.[3] [4] Following there were a lot of investigations to elucidate the electronic configuration of such a system. This comprise electronic, Raman and EPR spectroscopies and magnetic studies, [5-9] as well the synthesis of many other diruthenium tetracarboxylate compounds with different carboxylates and with different anions in axial positions [10-12] All studies agree with a delocalized mixed-valence type system ranging in the class III of the Robin-Day classification.[13] The electronic configuration has been established as $\sigma^2\pi^4\delta^2(\delta^*\pi^*)^3$ in the molecular orbital approach[7, 14]. That is, among the 11 electrons from the d^5 and d^6 configurations of the Ru(III) and Ru(II), 8 electrons fill the quadruple bond ($\sigma^2\pi^4\delta^2$) leaving three remaining unpaired electrons distributed in the π* and δ* orbitals, leading to a formal bond order of 5/2 in the ground configuration. The result is thus an unusual high-spin S=3/2 state for the whole diruthenium core. This is why it is better formulated as diruthenium(V) than diruthenium(II,III). In addition, the three unpaired electrons in the accidentally degenerated π* and δ* orbitals[2] cause a large zero-field splitting (D = 60-80 cm^{-1}) [2, 7, 9, 12, 15-17, 10-12].

The peculiar electronic structure of diruthenium tetracarboxylate compounds, combining a high-spin S=3/2 state with large ZFS together with the possibility to exchange the ligands in axial position, has prompted their use as building blocks of molecule-based magnets. One-, two- and three-dimensional systems have been reported built of diruthenium tetracarboxylate alone or bridged by paramagnetic linkers in axial position, such as nitroxide radicals or hexacyanidometalate ions $[M(CN)_6]^{3-}$ [10, 15, 18-21]. Among these systems, the one-dimensional chains present in the pivalate derivative $(PPh_4)_2[Ru_2(O_2C(CH_3)_3)_4W(CN)_8]$, previously reported by our group, exhibit a high ordering temperature (Tc = 44 K)[20] and represent one of the best examples of high-spin diruthenium(V) tetracarboxylate compounds. Improving the performance of these molecule-based magnets requires a detailed knowledge of magneto-structural

View Article Online
DOI: 10.1039/D6DT00342G

relationships at the molecular level, and this raises two main questions that we address in this paper.

A first question concerns the spatial distribution of the unpaired electron density, both between the ruthenium atoms, and how much it is delocalized onto the carboxylate and axial ligands. Early theoretical calculations have tentatively answered this question[7], and we also previously reported a ^{13}C NMR study which agreed with some spin delocalization onto the carboxylate groups.[22] We now revisit this question by probing the experimental mapping of the electron and spin distributions in one diruthenium(V) tetracarboxylate compound $(NBu_4)[Ru_2^V(O_2CCH_3)_4Br_2]$ using high-resolution X-ray diffraction (XRD) on single crystals and Polarized Neutron Diffraction (PND). High-resolution XRD is a powerful crystallographic technique which enables precise experimental model of electron density distributions within the crystal using a multipole refinement.[23-25] The resulting deformation density, that is the deviations from the spherical atom model, allows for visualization of the bonding and charge localization.[26] This may be complemented by calculating the Laplacian ($\nabla^2\rho$) of the electron density to highlight regions of charge concentration and depletion, to have an insight into bond character.[27] Also complementary, the topological analysis based on quantum theory of atoms in molecules (QTAIM) [28] identifies especially critical points corresponding to bonding interactions and give access to atomic charges.[29] A full multipolar model can also give access to a precise calculation of the electrostatic potential, providing insights into interatomic electrostatic interactions, including energetic aspect.[30] PND on single crystal is another powerful crystallographic technique to probe magnetic compounds at the atomic level.[31] PND proved to be particularly powerful to map the spin density in molecular and coordination compounds, where it may spread outside of magnetic centres, such as in ligands.[32] Beyond this, PND provides direct information on the relationships between the crystal structure and the magnetic interactions pathways.[33-37]

A second important question, with diruthenium tetracarboxylate compounds, is how large is the molecular magnetic anisotropy and how are oriented its principal magnetic axis with respect to the molecular geometry. This determines how large could be the remnant magnetization and the coercive field of the molecule-based magnets[38, 39]. As molecular magnetic anisotropy is related to the ZFS, we know the molecular magnetic anisotropy is large in these diruthenium(V) tetracarboxylate compounds, and its size may be measured by different experimental techniques such as electron paramagnetic resonance (EPR).

View Article Online
DOI: 10.1039/D6DT00342G

However, determination of the principal magnetic axis orientation is tricky. To address this question we used also PND data on single crystal within the local susceptibility tensor approach[40]. We have shown previously that this allows the fine determination of the direction and strength of the local principal magnetic anisotropy axes on the metal ions[41-46]. Supported by quantum mechanical calculations, our results reveal an unprecedented view of the charge and spin distribution as well the magnetic anisotropy in diruthenium tetracarboxylate systems.

Results and Discussion

We started the study with the tetra-pivalate diruthenium dithiocyanato compound, $[NBu_4][Ru_2^V(O_2C(CH_3)_3)_4NCS_2]$,[20] then the tetra-acetate dichloro derivative, $[NBu_4][Ru_2^V(O_2CCH_3)_4Cl_2]$.[22] Both could be grown as large single crystals suitable for PND. However, they incorporated crystallization solvents that escaped during the experiments, preventing reliable data collection. Driven by our continued interest in diruthenium tetracarboxylate systems, we then turned to the n-butyrate derivative with bromido ligands in the axial positions, which finally yielded large solvent-free single stable crystals of (NBu_4) $[Ru_2^V(O_2CCH_3)_4Br_2]$ enabling successful neutron diffraction measurements. Moreover, this compound is one of the few diruthenium tetracarboxylates featuring bromido ligands.[47-51]

High-resolution X-Ray diffraction crystal structure: Tetra-*n*-butylammonium tetra-*n*-butyratodibromidodiruthenium $(NBu_4)[Ru_2^V(O_2CC_3H_7)_4Br_2]$ crystallises in the triclinic $P\bar{1}$ space group. Crystal data and structure refinement parameters, obtained from high-resolution XRD on single crystal at 100K, are summarised in Table S1. The asymmetric unit comprises two halves of centrosymmetric diruthenium anion complexes $[Ru_2^V(O_2CC_3H_7)_4Br_2]^-$ labelled A and B and one tetra-*n*-butylammonium counter-cation (NBu_4) for electroneutrality. One terminal carbon atom (C4) of a butyl chain of the tetrabutylammonium cation (NBu_4) was refined as disordered on two positions. Each of the tetra-*n*-butyratodirutheniumdibromido anion complex units $[Ru_2^V(O_2CC_3H_7)_4Br_2]^-$, A and B, have a crystallographic inversion centre at the midpoint of the diruthenium core with the two equivalent ruthenium ions coordinated in the equatorial plane by four bridging tetra-*n*-butyrato ligands in the so-call paddlewheel fashion. As shown on Figure 1 and Figure S1 for unit A and B, bromido ligands complete the coordination of both ruthenium ions in axial position. The major difference between dinuclear units A and B

View Article Online
DOI: 10.1039/D6DT00342G

lies in the conformation of the *n*-butyl chains of the *n*-butyrato ligands, which show the *cis* and *trans*-conformation for A, but only the *trans*-conformation for B (Figure S2). The structural features are very close to those reported by Cotton for the first tetracarboxylato diruthenium complex as well for other tetracarboxylato diruthenium complexes.[2] The four oxygen atoms, located in the equatorial plane of each ruthenium, are strictly coplanar and the ruthenium ions are slightly out of the plane (Ru1A: 0.035Å, Ru1B: 0.033Å). Consistent with earlier studies the Ru-Ru distances exceed the mean O-O distance in the carboxylate group (Table S2) and are in the range of those observed for diruthenium(II,III) tetaracarboxylato complexes (2.27—2.31 Å). [10-12, 47-51] The Ru-Br bond lengths (Table S2) are similar to those in other tetracarboxylatodibromidodiruthenium complexes.[47-51] Comparatively they are larger than the Ru-Br bond lengths usually observed in bromido complexes of Ru^{3+} and Ru^{2+} complexes. This makes the substitution of the axial ligands easy as early pointed by Cotton.[2] Moreover, the Ru-Br bonds in the dibromido isolated complexes are comparatively shorter than those of the bromido-bridged chain complexes making the Ru-Ru distances in dibromido isolated complexes (2.2998(19)-2.3124(11) Å) a little longer than those found in bromido-bridged chain compounds (2.2850(6)-2.2906(7) Å).[47-51]

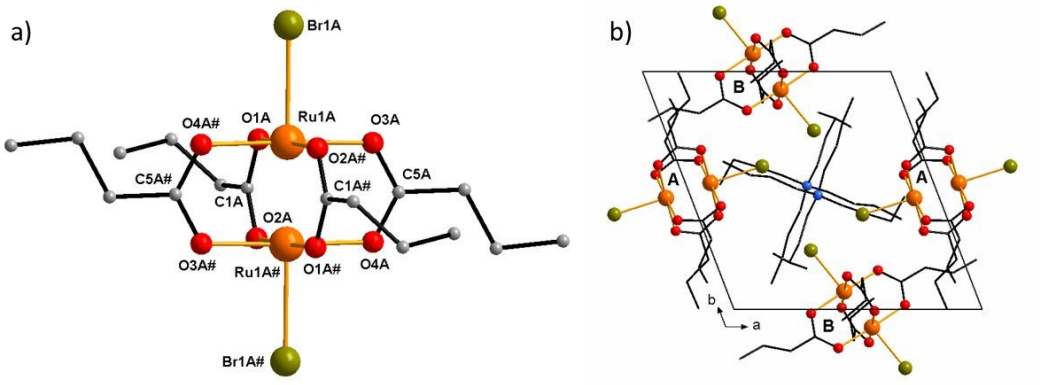

Figure 1: a) Representation showing the $[Ru_2^{V}(O_2CC_3H_7)_4Br_2]^-$ anion complex unit labelled A. b) View along the **c** axis of diruthenium A and B in unit cell. Hydrogen atoms are omitted for clarity.

Electron density model: The static deformation density maps calculated as the difference between the multipolar and independent atom models show positive

View Article Online
DOI: 10.1039/D6DT00342G

deformation densities along the C-O and C-C bonds of the carboxylate ligand as expected (Figure 2a and Figure S3a-d)[52]. For both diruthenium complexes A and B, the lone pairs of the oxygen atoms are pointing toward ruthenium centre. We can notice (Figure 2a and Figure S3) an accumulation of the charge density of the ligands pointing toward depletion at the metal centres as has been reported for other metal complexes and in agreement with the concept of donor-acceptor ligand-metal bond.[26, 53, 54] The charge density over each of the ruthenium centres is similar in both A and B diruthenium complexes and has a cross shape comprising six negative lobes and four positive lobes (Figure S4). Five negative lobes point toward the ligands while the sixth is pointing directly toward the Ru---Ru bond. The four positive lobes (Figure S3e-f) have diagonal directions (Figure S4). Looking at the Ru---Ru bond there is no sizeable charge accumulation.[55]

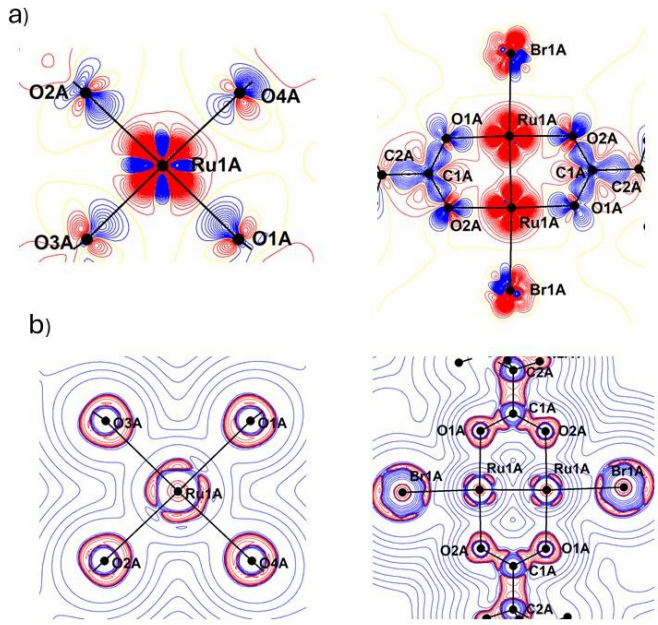

Figure 2: a) Static deformation density map of dimer A (blue = positive, red = negative, yellow = zero contour). Isocontour lines are separated by 0.05 e/A^3. b) Laplacian of the electron density of diruthenium A (blue = positive, red = negative; contour at ±2, 4, 8×10^n with n = -1, 0, 1, 2).

The Laplacian maps (Figure 2b, Figure S5) clearly evidence the valence shell charge concentrations (VSCC) and valence shell charge depletions (VSCD). The C–O bond shows the expected feature of a normal covalent bond[52] and the valence shell charge concentration (VSCC) of a carbon and oxygen atom is indicated as an sp^2 valence

View Article Online
DOI: 10.1039/D6DT00342G

configuration. The donor character of the lone pair toward the Ru atom is confirmed by the charge concentrations of oxygen atoms, as expected for a metal-ligand coordination bond.[52] For both A and B diruthenium complexes there are four VSCCs and six VSCDs around each Ru atom, visible on Figure 2b, Figure S5a-d with the VSCCs located in between the Ru–O bond directions.[55] The valence shell of the ruthenium atoms reflects the uneven population among the five d-orbitals and indicates the preferred population on t_{2g} and e_g orbitals.[54, 56]

The topological analysis of the electron density[29] of Ru-O and Ru-Br interactions is in agreement with polar covalent bonds (Table S5). Considering the middle of the bonds, the positions of the bonds critical points (BCPs) of the Ru-O bonds have an average shift of 0.7 Å away from Ru atoms and toward O atoms, indicating a slight polarization.[53] The metal-ligand bonds have similar topological properties at BCPs with an average density ρ =0.32 e.Å^{-3} for Ru-Br and ρ = 0.70 e.Å^{-3} for Ru-O, with positive Laplacian ($\nabla^2\rho$ = 3.9 e.Å^{-5} for Ru-Br and $\nabla^2\rho$ = 11 e.Å^{-5} for Ru-O). The value of the ellipticity $\boldsymbol{\varepsilon}$ with an average of 0.01 for Ru-Br and 0.12 for Ru-O is in agreement with a single covalent bonding. The topological properties of the Ru-L bonds are comparable to those of other related metal-ligand interactions. [53, 54, 57] For the Ru---Ru interactions, the BCP is localized at the midpoint between the two ruthenium atoms. The small value of the electron density at BCP (ρ=0.50 e.Å^{-3}), the positive value of the Laplacian ($\nabla^2\rho$ = 8.3 e.Å^{-5}), the positive value of G_{cp}/ρ (0.19 he^{-1}) but smaller than unity and the small negative value of G_{cp}/ρ (-0.02 he^{-1}) are consistent with an open-shell metal-metal interaction.[58, 59] The high value of the Laplacian ($\nabla^2\rho$ > 1 e.Å^{-5}) appears inadequate for the classification of the M-M bond, but increase of the Laplacian at the BCP as already reported for metal–metal bond orders greater than unity.[60, 61] An experimental value of $\nabla^2\rho$ = 31.62 e.Å^{-5} has also been reported in the study of quintuply-bonded dichromium complex $Cr_2(dipp)_2$.[52]

The complementary analyses of the experimental electron density in $(NBu_4)[Ru_2^V(O_2CC_3H_7)_4Br_2]$, derived from high-resolution XRD, provide a detailed mapping of the electron distribution that agrees well with previous studies on tetracarboxylato diruthenium(V) complexes and a delocalized class III mixed-valence system in the Robin-Day classification.[13] The electron distribution in both A and B diruthenium moiety was found to be largely similar, as were atomic charges (Table S4). The main difference was found in refinement of the parameter κ' (Table S3), which converged to a slightly higher value for Ru1B (1.41) than for Ru1A (1.20). Since the κ

View Article Online
DOI: 10.1039/D6DT00342G

and κ' parameters control the radial expansion/contraction of the outer shell within the multipole model, this higher value for Ru1B reflects a more contracted outer shell than Ru1A.[23-25] It is all the more notable that this is consistent with a similar difference between Ru1A and Ru1B that we observed in the refinement of magnetic anisotropy from the PND data reported below.

Magnetic studies: Magnetic measurement on a polycrystalline sample gave a value of the product of magnetic susceptibility with temperature (χT) of 2.16 $cm^3\,K\,mol^{-1}$ at 300 K (Figure 3a). This is close to the spin-only value for three unpaired electrons (χT= 1.875 $cm^3\,K\,mol^{-1}$) in accordance with the electron configuration of $\sigma^2\pi^2\delta^2(\pi^*\delta^*)^3$. Upon cooling the χT product decreases continuously down to 1.40 $cm^3\,K\,mol^{-1}$ at 2 K (Figure 3a).

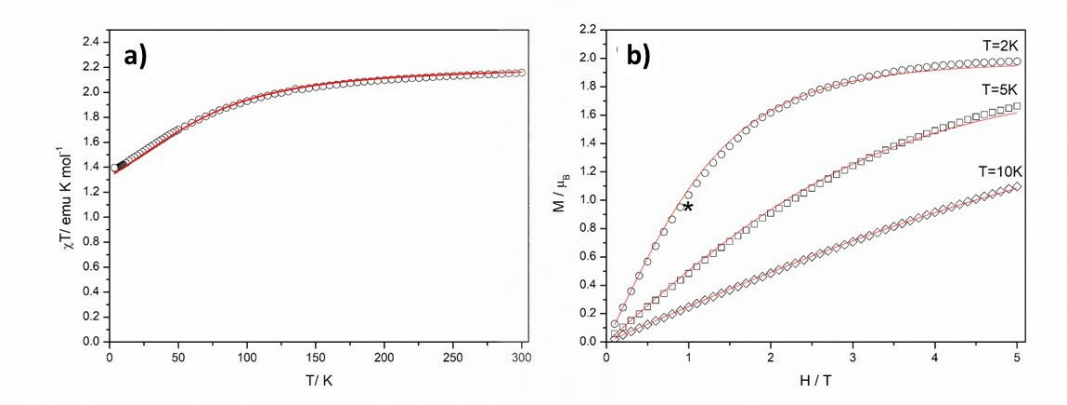

Figure 3: a) Experimental (○) temperature dependence of $\chi_M T$ of **1** and b) field dependence of the magnetization at 2K (○), 5K (□□) and 10K (◊).The red solid lines denotes the simulated value with parameters of g = 2.13, D = 83 cm^{-1}, and zJ = 0 cm^{-1}. The magnetization estimated by the local susceptibility tensors measured from PND data is shown by a star symbol.

The magnetic data were well simulated using the conventional method with parameters, g = 2.16 and D = 83 cm^{-1} and the previously reported analytical expressions for diruthenium tetracarboxylate. [18] These values are similar to those reported for other lantern-type diruthenium(V) complexes[9, 12, 15-17]. Implementation of intermolecular interaction between the diruthenium complexes, in the molecular field approximation (zJ),[12, 62] did not improve the quality of the fit and was considered negligible as within the crystal the closest intermolecular Ru···Ru distance is 8.2935(11)Å. The field

View Article Online
DOI: 10.1039/D6DT00342G

dependences of the magnetization at different temperatures are also well simulated (Figure 3b) with these parameters.

Further angle-resolved susceptibility measurements were performed on one single crystal of 3.5×2.5×1.5 mm^3 at 2K under a magnetic field of 0.1T as shown in Figure S6. Rotation of the crystal around the ***a*** and ***b*** crystallographic axes perpendicular to the magnetic field clearly shows the existence of a significant magnetic anisotropy with the easy magnetization axis preferentially along the ***c*** axis. The hard magnetization axis is mainly along the ***b*** axis. However, due to the presence of two dimers A and B in the unit cell, the molecular magnetic principal axes of each dimer cannot be deduced from these angle-resolved measurements.

Spin density model: Study of the spin density was carried out by polarised neutron diffraction (PND) as the best method to gain insight into the possible delocalisation of unpaired electrons towards the ligands and between the ruthenium atoms. Flipping ratios were collected on D3 diffractometer at Institute Laue Langevin (ILL) at 2K under an applied magnetic field of 9T.[31] The nuclear structure factors were obtained from neutron diffraction measurements performed at the same temperature on D19 diffractometer at ILL.

PND data were analysed using the model-free Maximum Entropy Method (MEM), which is known to give much more reliable results than conventional Fourier syntheses by significantly reducing both noise and truncation effect.[63, 64] However, it should be noted that in magnetically anisotropic compounds, MEM only reconstructs the component of the magnetization density along the applied magnetic field, which only allows for qualitative localization of unpaired electrons in the unit cell. As the local symmetry of the magnetic ion is the same as the overall symmetry of the crystal, the same symmetry paramagnetic group $P\bar{1}$ has been used in the reconstruction of spin density. The results of the reconstruction are presented in Figure 4 and Figure S7**.**

View Article Online
DOI: 10.1039/D6DT00342G

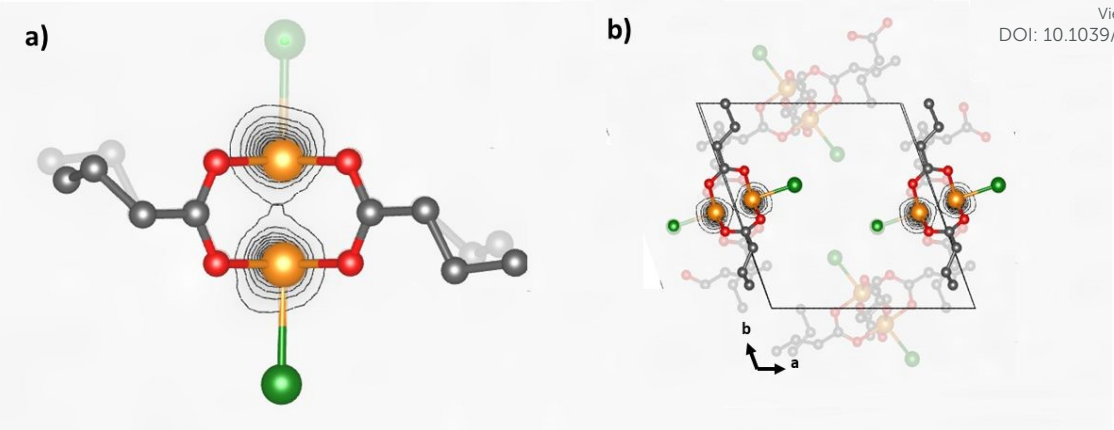

Figure 4: Experimental spin density at 2 K under a field of 9 T applied nearly along the *c*-axis for diruthenium A a) projection around the Ru-Ru bond. b) Projection of the unit cell along the [001] direction. Contour levels are fixed at $0.035\mu_B/A^3$.

From distribution measured in saturated regime it appears that spin density is mainly located on the Ru atoms of the diruthenium complexes (Figure 4 and Figure S7) with almost no significant spin densities on the ligands.

Magnetic susceptibility tensor: PND was also used to determine the local magnetic anisotropy by the local susceptibility tensor method.[40, 44] In these experiments, flipping ratios were collected on the D3 diffractometer at ILL at 2K under a magnetic field of 1T and for three different orientations of the crystal from which the magnetic susceptibility tensors of each Ru ion of the two A and B diruthenium complexes were determined:

$$\boldsymbol{\chi_{RuA}} = \begin{pmatrix} \mathbf{0.25(3)} & \mathbf{0.03(3)} & \mathbf{0.02(2)} \\ \mathbf{0.03(3)} & \mathbf{0.64(7)} & \mathbf{-0.01(2)} \\ \mathbf{0.02(2)} & \mathbf{-0.01(2)} & \mathbf{0.65(1)} \end{pmatrix} \frac{\boldsymbol{\mu_B}}{\boldsymbol{T}}$$

$$\boldsymbol{\chi_{RuB}} = \begin{pmatrix} \mathbf{0.61(3)} & \mathbf{0.09(3)} & \mathbf{-0.04(2)} \\ \mathbf{0.09(3)} & \mathbf{0.07(7)} & \mathbf{0.10(2)} \\ \mathbf{-0.04(2)} & \mathbf{0.10(2)} & \mathbf{0.66(1)} \end{pmatrix} \frac{\boldsymbol{\mu_B}}{\boldsymbol{T}}$$

The tensors are defined in the right-hand Cartesian coordinate system XYZ: $\boldsymbol{Z}$ is along the crystallographic axis $\boldsymbol{c}$ and $\boldsymbol{X}$ is along the reciprocal crystallographic axis $\boldsymbol{a^*}$. The experimental error bars are given in brackets. They are represented in the form of magnetization ellipsoids in Figure 5. This clearly shows a planar-type anisotropy oriented towards the oxygen planes for both dimers and indicates a significant influence of oxygen on the magnetic anisotropy of Ru ions.

View Article Online
DOI: 10.1039/D6DT00342G

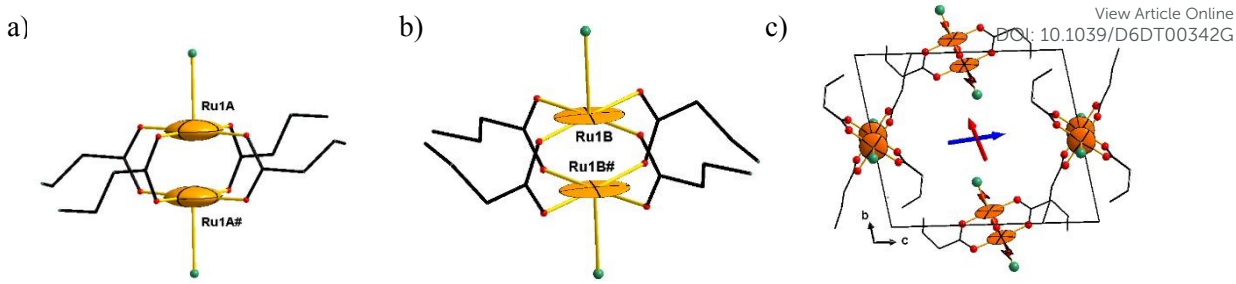

Figure 5: Magnetization ellipsoids on Ru site measured at 2K 1T in unit cell. Orientation of magnetization ellipsoid according the molecular frame is shown for the dimer A (a) and the dimer B (b). The easy and hard magnetization axes of the sample are indicated by blue and red arrows, respectively (c).

Diagonalization of magnetic susceptibility tensors give the following eigenvalues for the main axes of Ru1A and Ru1B magnetic anisotropy:

$$\chi_{A1} = 0.24\ \mu_B T^{-1},\ \chi_{A2} = 0.64\ \mu_B T^{-1},\ \chi_{A3} = 0.65\ \mu_B T^{-1}$$

$$\chi_{B1} = 0.04\ \mu_B T^{-1},\ \chi_{B2} = 0.62\ \mu_B T^{-1},\ \chi_{B3} = 0.69\ \mu_B T^{-1}$$

This confirms the planar magnetic anisotropy, which is almost "flat" for Ru1B, with the easy plane in the oxygen plane being around 0.65 $\mu_B T^{-1}$ for Ru1A and Ru1B, and a small transverse susceptibility for Ru1A (χ_{A1} =0.24 $\mu_B T^{-1}$) but almost zero for Ru1B (χ_{B1} = 0.04 $\mu_B T^{-1}$).

Based on the refined susceptibility tensors the estimated easy magnetization axis of the crystal is oriented mainly along the crystallographic axis $\boldsymbol{c}$: $-0.01\boldsymbol{X} + 0.15\boldsymbol{Y} + 0.99\boldsymbol{Z}$ (blue arrow in Figure 5c), while the hard magnetization axis is mainly oriented along the $\boldsymbol{b} - \boldsymbol{a}$ direction: $-0.46\boldsymbol{X} + 0.88\boldsymbol{Y} - 0.14\boldsymbol{Z}$ (red arrow in Figure 5c).

From the summation of tensors, χ_{RuA} and χ_{RuB}, the angular resolved susceptibility and magnetization of the sample have been calculated (see details in the supporting information). The estimated sample magnetization at the applied field (1T) along the main crystallographic axis agrees well with magnetic measurement in terms of error bars (Figure S6b). Simulation of angular-resolved susceptibility demonstrates quite a good agreement with experimental data measured at 0.1 T (Figure S6a).[42] The orientations of the easy and hard magnetization axes are predicted correctly. The small disagreement in absolute values between predictions and experiment relates to the fact that the magnetization curve is outside of the linear region at field 1T at which the PND

View Article Online
DOI: 10.1039/D6DT00342G

measurements have been performed. The calculated powder averaged magnetization ($0.48(7)\ \mu_B$/ion) is in excellent agreement with the magnetization measured on the powder sample at 2K (Figure 3b). Thus, the local susceptibility tensors measured by PND well describe the magnetometry data.

It is important to emphasize that such a precise determination of the magnetic anisotropy is not possible by magnetometry. Only the PND can provide the local susceptibility tensors and the anisotropy on each magnetic ruthenium centre. Thus, if one would consider the mixed-valence diruthenium as being localised, class I or class II of the Robin-Day classification, with one Ru^{2+} and one Ru^{3+}, their magnetic moments would be significantly different and could be distinguishable by PND. Moreover, such ordering would break the inversion symmetry of the dimer, leading to the loss of the symmetry centre. Nevertheless, decreasing the space group to $P1$ does not improve the quality of refinement. This is another confirmation that in each diruthenium the two ruthenium atoms are equivalent in full agreement with previous reports and with analysis of charge density distribution.[1-12, 14]

However, although the two ruthenium atoms in each diruthenium are equivalent, there are differences between the two diruthenium units also in their (de)localised character. As we have just seen, although the anisotropy of Ru1A and Ru1B are both planar, that of Ru1B is much flatter (Figure 5). Indeed, as with the determination of electron density, refinement of the magnetic anisotropy of ruthenium results in $\kappa Ru1A$=1.03(1) and $\kappa Ru1B$=1.17(2) which indicates that it is slightly more contracted for diruthenium B than for diruthenium A. Given that the studies were conducted independently and on different crystals, a small one for charge density and large one for magnetic anisotropy, we believe that this difference between Ru1A and Ru1B is meaningful. Thus the contraction effect we observed in both experiments for Ru1B suggests that diruthenium B may be a slightly more localized than diruthenium A. In other words while still a delocalised mixed-valence of class III, with spin S=3/2 in agreement with magnetism, diruthenium B may be somewhat closer to a localised case, as has been argued for some other borderline mixed-valence complexes.[65]

View Article Online
DOI: 10.1039/D6DT00342G

Quantum mechanical calculations: The fine description of the nature of many-electron states in transition metal complexes may require the use of multiconfigurational quantum mechanical calculations. For the sake of having a qualitatively correct view on the bonding pattern in the complex of interest and also for an accurate description of the (molecular) anisotropy of the complex, we have therefore only employed multiconfigurational and multireference wave function approaches (see Supporting Information for the computational details).

We start our analysis by a bonding analysis in terms of effective bond order.[66] As mentioned in the introduction, the ground electronic configuration in the valence space of the two ruthenium centres is $\sigma^2\pi^4\delta^2(\delta^*\pi^*)^3$, which corresponds to a formal bond order of 5/2 (8 bonding and 3 antibonding electrons). A state-specific complete active space self-consistent field (CASSCF) calculation based on 11 electrons to be spread amongst those 10 valence d orbitals of the metals for the ground quartet spin state allows one to revise this formal bond order to define an effective one. The electronic configuration of the ground state being $\sigma^{1.88}\pi^{3.76}\delta^{1.85}\delta^{*1.14}\pi^{*2.22}\sigma^{*0.12}\delta^{0.01}\delta^{*0.01}$ at the CASSCF level, an effective bond order of 2.01 is found. The σ (0.88) and π (0.77) contributions to this bond order are in perfect line with what was previously found in diruthenium(II) cases,[67] the extra electron withdrawal here favour the emergence of a δ partial bond (0.36), resulting in a higher (effective) bond order. These results arise from calculation on diruthenium A. Results for diruthenium B are reported in Supplementary Information. No significant changes are observed in the computed properties of diruthenium B as may be expected because the two complexes (A and B) show minor structural differences (calculations were based on the experimental crystallographic structure).

Table 1: Atomic spin densities obtained at the CASSCF level and from spin-unrestricted DFT calculations with the B3LYP exchange-correlation functional.

complex		Ru	Br	O	C (carboxylate)
A	CASSCF	1.438	0.014	0.010 ; 0.011	0.003
	B3LYP [68-70]	1.379	0.065	0.028 ; 0.030	–0.029
B	CASSCF	1.438	0.013	0.010 ; 0.011	0.003
	B3LYP [68-70]	1.381	0.062	0.028 ; 0.030	–0.029 ; –0.030

View Article Online
DOI: 10.1039/D6DT00342G

The Mulliken atomic spin densities have then been determined for this ground spin-orbit Free State at the CASSCF level and from spin-unrestricted DFT calculations with B3LYP 24-26. [68-70] As expected, the spin density delocalizes more at the spin-unrestricted B3LYP level compared to what is observed at the CASSCF level. Nevertheless, both evidence a larger spin delocalization on each Br atom than on each O atom, meaning that these results are robust with respect to the applied quantum mechanical method.

It turns out that the spin density is essentially localized on the Ru atoms (1.438 each), and then moderately propagated on the ligands (0.014 per Br atom, 0.011 per O atom, and 0.003 on each C atom bridging two coordinated O atoms). No distinction can be made between the two Ru atoms from the atomic spin densities: the system effectively behaves as a typical class III mixed-valence compound. Note that although the atomic charges are strongly dependent on the underlying charge model and also level of theory, the atomic spin populations are by experience less dependent on those choices and that therefore the observed trend (more delocalization on the Br *vs.* O atoms) is not expected to be biased by them.

In view of further computing the zero-field splitting of the ground $S = 3/2$ state by means of the established spin-orbit configuration interaction technique combined with the effective Hamiltonian theory,[71] we have computed several excited spin-orbit free states. A good compromise between accuracy, computational cost, and limitation of state-averaging artefact was found for a set of 13 $S = 3/2$ and 16 $S = 1/2$ spin-orbit free states (see Supporting Information for more details). At the N-electron valence state second-order perturbation theory (NEVPT2) level,[72, 73] the ground $S = 3/2$ state lies 0.91 eV below the first excited $S = 3/2$ state and 0.29 eV below the first (excited) $S = 1/2$ one. Once the spin-orbit coupling is introduced, the lowest-two Kramers doublets are split by 188 cm^{-1} (23.2 meV) and the extracted zero-field splitting parameters are $D = 94$ cm^{-1} and $E = 2$ cm^{-1}, in good agreement with experiment. The hard axis of magnetization almost perfectly coincides with the Ru–Ru orientation, which is unsurprising given the paddlewheel structure. Furthermore, the composition of the lowest-two Kramers doublets being largely dominated by the spin components of the ground spin-orbit free state (96.6% and 99.1%, respectively), no significant reduction of the effective bond order by the spin-orbit coupling[74] is here expected, meaning that the previous effective bond order picture holds: the system is thus indeed the subject of an effective double bond.

View Article Online
DOI: 10.1039/D6DT00342G

Conclusion

Study of the spin density by PND and the electron density by high-resolution XRD, supported by ab initio calculation, provide complementary insights of the electronic and magnetic structure of the mixed-valent diruthenium(V) tetracarboxylate complex. The charge-density maps show the distribution of electron density, which is mainly localised on the ruthenium centres, with no significant density in between. However, they also indicate some delocalisation from the ruthenium centres towards the bromido and carboxylato ligands. Experimental topological analysis of the Ru---Ru bond shows an open-shell metal-metal interaction, in agreement with the $\sigma^2\pi^4\delta^2(\pi^*\delta^*)^3$ electronic configuration. In contrast, the spin-density maps show that the unpaired electrons are predominantly localized on the ruthenium atoms. Considering that quantum calculations indicate similar delocalized spin populations on both oxygen and bromido ligands, these observations suggest that the delocalized spin density lies beyond the detection limit of our PND experiment.

The local magnetic susceptibility tensors derived from PND show planar anisotropy aligned with the equatorial oxygen atoms and a hard axis along the Ru–Ru bonds, highlighting the strong influence of oxygen geometry on the anisotropy. These observations are fully consistent with bulk magnetic data, which show an easy magnetization axis along the crystallographic ***c*** axis and a hard axis along ***b***, but provide a more detailed, atomically resolved description of the magnetic anisotropy.

Moreover, the experimental electron density from high-resolution XRD and the experimental magnetic anisotropy from PND show that the valence shell of diruthenium B is more contracted and lead to hypothesize diruthenium B as a slightly more localized mixed-valence than diruthenium A but, still, a delocalised mixed-valence of class III with spin S=3/2. This result demonstrates the value and power of such a study, combining advance crystallographic methods for the determination of experimental electron and spin densities and magnetic anisotropy, which reveal such details that could not be obtained from a classical crystallographic structure even combined with magnetometry measurements.

View Article Online
DOI: 10.1039/D6DT00342G

Author contributions

Haruki Yairi and Torao Fujimoto: Investigation

Sabrina Grenda, Oscar Fabelo, Iurii Kibalin, Nicolas Claiser, Rémi Maurice, Arsen Gukasov, Laura Canadillas-Delgado, José A. Rodriguez Velamazan, Jean-François Jacquot, Ryoji Mitsuhashi, Masahiro Mikuriya, Makoto Handa: Investigation, writing, reviewing & editing

Dominique Luneau: Supervision, investigation, writing, reviewing & editing

Conflicts of interest

There are no conflicts to declare.

Data availability

Electronic supplementary information (ESI) available report experimental details on synthesis, characterization and crystal growing of (NBu_4) $[Ru_2^{V}Br_2(O_2CCH_3)_4]$, High-resolution X-Ray diffraction crystal structure, Experimental electron density model, Magnetic measurements, Neutron diffraction, Polarized neutron diffraction, Experimental spin density model and magnetic susceptibility tensors determination, Quantum mechanical calculations complemented by additional Tables and Figures for crystal structures electron density, spin density and magnetism; The crystallographic information files (CIF), containing the X-ray crystallographic data with embedded multipole model and experimental structure factors and non-polarised neutron data has been deposited at The Cambridge Crystallographic Data Centre,12 Union Road, Cambridge CB2 1EZ, UK; fax: +44 1223 336 033. (CCDC deposition number 2516707 and 2519322). The authors have cited additional references within Supporting Information.[23, 42, 66, 71-73, 75-90]

Acknowledgements

Dedication: The authors dedicate this paper to Beatrice Gillon for her seminal work in polarised neutron diffraction of magnetic coordination compounds.

Low-temperature high-resolution X-Ray diffraction on single-crystal was carried out at the PMD2X X-ray diffraction facility of the CRM2 laboratory (Université de Lorraine) for (https://www.crm2.univ-lorraine.fr/plateformes/pmd2x/). Polarised and non-polarized neutron diffraction experiments were performed on the D3 and D19 diffractometers respectively, run by the Institut Laue-Langevin (ILL); beamtime was granted under the proposals number 5-51-584 (DOI: 10.5291/ILL-DATA.5-51-584) and

View Article Online
DOI: 10.1039/D6DT00342G

5-51-564 (DOI: 10.5291/ILL-DATA.5-51-564) We thank Dr. Frédéric Guégan for discussion and participation in preliminary data collection. This work was partially supported by JSPS KAKENHI Grant Number JP24K08363 and Region Auvergne-Rhône-Alpes and its programme "Ambition Internationale 2025" Grant number 00283799-1.

Footnotes

[#] Present addresses: **Iurii Kibalin:** European Spallation Source ERIC, P.O. Box 176, SE-221 00 Lund, Sweden; **Ryoji Mitsuhashi:** Institute of Liberal Arts and Science, Kanazawa University, Kakuma, Kanazawa 920-1192, Japan

References

1. T. A. Stephenson and G. Wilkinson, New Ruthenium Carboxylate Complexes, *J. Inorg. Nucl. Chem.*, 1966, **28**, 2285-2291.
2. M. J. Bennett, K. G. Caulton and F. A. Cotton, Structure of Tetra-N-Butyratodiruthenium Chloride a Compound with a Strong Metal-Metal Bond, *Inorg. Chem.*, 1969, **8**, 1-6.
3. F. A. Cotton, N. F. Curtis, B. F. G. Johnson, J. T. Mague, J. S. Wood, C. B. Harris, W. R. Robinson and S. J. Lippard, Mononuclear + Polynuclear Chemistry of Rhenium (3) - Its Pronounced Homophilicity, *Science*, 1964, **145**, 1305-1307.
4. F. A. Cotton and D. G. Nocera, The whole story of the two-electron bond, with the delta bond as a paradigm, *Acc. Chem. Res.*, 2000, **33**, 483-490.
5. R. J. H. Clark and M. L. Franks, Resonance Raman-Spectra of Chlorotetra-Acetato-Diruthenium and Chlorotetrabutyrato-Diruthenium., *Dalton Trans.*, 1976, 1825-1828.
6. F. A. Cotton and E. Pedersen, Magnetic and Electrochemical Properties of Transition Metal Complexes with Multiple Metal-to-Metal Bonds. II. $[Ru_2(C_3H_7COO)_4]^{n+}$ with *n = 0 and 1*, *Inorg. Chem.*, 1975, **14**, 388-391.
7. J. G. Norman, G. E. Renzoni and D. A. Case, Electronic-structure of $Ru_2(O_2CR)_4^+$ and $Rh_2(O_2CR)_4^+$ complexes, *J. Am. Chem. Soc.*, 1979, **101**, 5256-5267.
8. C. R. Wilson and H. Taube, Acetate Complexes of Dirhodium and Diruthenium - Aquation and Reduction-Oxidation., *Inorg. Chem.*, 1975, **14**, 2276-2279.
9. J. Telser and R. S. Drago, Reinvestigation of the Electronic and Magnetic-Properties of Ruthenium Butyrate Chloride, *Inorg. Chem.*, 1984, **23**, 3114-3120.
10. M. A. S. Aquino, Diruthenium and diosmium tetracarboxylates: synthesis, physical properties and applications, *Coord. Chem. Rev.*, 1998, **170**, 141-202.
11. P. Angaridis, in *Multiple Bonds Between Metal Atoms*, eds. F. A. Cotton, C. A. Murillo and R. A. Walton, Springer US, Boston, MA, 2005, pp. 377-430.
12. M. Mikuriya, D. Yoshioka and M. Handa, Magnetic interactions in one-, two-, and three-dimensional assemblies of dinuclear ruthenium carboxylates, *Coord. Chem. Rev.*, 2006, **250**, 2194-2211.
13. M. B. Robin and P. Day, Mixed Valence Chemistry-A Survey and Classification, *Adv. Inorg. Chem. Radiochem.*, 1968, **10**, 247-422.
14. L. R. Falvello, B. M. Foxman and C. A. Murillo, Fitting the Pieces of the Puzzle: The delta Bond, *Inorg. Chem.*, 2014, **53**, 9441-9456.

15. M. Handa, Y. Sayama, M. Mikuriya, R. Nukada, I. Hiromitsu and K. Kasuga, Structure and magnetic properties of a chain complex with alternating Ru(II,III) dimer and nitroxide radical arrangement Ru-2(O2CCMe3)(4)(nitph) (n)(BF4)(n), nitph = 2-phenyl-4,4,5,5-tetramethyl-4,5-dihydro-1H-imidazol-1-oxyl 3-N-oxide, *Bull. Chem. Soc. Jpn*, 1998, **71**, 119-125.
16. F. D. Cukiernik, D. Luneau, J. C. Marchon and P. Maldivi, Mixed-valent diruthenium long-chain carboxylates. 2. Magnetic properties, *Inorg. Chem.*, 1998, **37**, 3698-3704.
17. R. Jimenez-Aparicio, F. A. Urbanos and J. M. Arrieta, Magnetic properties of diruthenium(II,III) carboxylate compounds with large zero-field splitting and strong antiferromagnetic coupling, *Inorg. Chem.*, 2001, **40**, 613-619.
18. W. W. Shum, Y. Liao and J. S. Miller, Zero-field splitting, field-dependent magnetization of mixed-varent S = 3/2 diruthenium(II,III) tetracarboxylates, *J. Phys. Chem. A*, 2004, **108**, 7460-7462.
19. M. Mikuriya, K. Tanaka, M. Handa, I. Hiromitsu, D. Yoshioka and D. Luneau, Adduct complexes of ruthenium(II,III) propionate dimer with pyridyl nitroxides, *Polyhedron*, 2005, **24**, 2658-2664.
20. M. Mikuriya, D. Yoshioka, A. Borta, D. Luneau, D. Matoga, J. Szklarzewicz and M. Handa, Molecule-based magnetic materials based on dinuclear ruthenium carboxylate and octacyanotungstate, *New. J. Chem.*, 2011, **35**, 1226-1233.
21. M. Mikuriya, D. Yoshioka, D. Luneau, S. Kawauchi, D. Matoga, J. Szklarzewicz and M. Handa, Tetra(n-butyl)ammonium salt of a ferrimagnetic complex based on mixed-valent dinuclear ruthenium pivalate and octacyanidotungstate(V), *C R Chim*, 2019, **22**, 476-482.
22. Y. Hiraoka, T. Ikeue, H. Sakiyama, F. Guegan, D. Luneau, B. Gillon, I. Hiromitsu, D. Yoshioka, M. Mikuriya, Y. Kataoka and M. Handa, An unprecedented up-field shift in the ^{13}C NMR spectrum of the carboxyl carbons of the lanterntype dinuclear complex TBA[$Ru_2(O_2CCH_3)_4Cl_2$] (TBA+ = tetra(n-butyl)ammonium cation), *Dalton Trans.*, 2015, **44**, 13439-13443.
23. N. K. Hansen and P. Coppens, Testing aspherical atom refinements on small-molecule data sets, *Acta Cryst. A*, 1978, **34**, 909-921.
24. P. Macchi, Modern charge density studies: the entanglement of experiment and theory, *Crystallogr. Rev.*, 2013, **19**, 58-101.
25. P. Macchi, J. M. Gillet, F. Taulelle, J. Campo, N. Claiser and C. Lecomte, Modelling the experimental electron density: only the synergy of various approaches can tackle the new challenges, *IUCrJ*, 2015, **2**, 441-451.
26. L. J. Farrugia, P. R. Mallinson and B. Stewart, Experimental charge density in the transition metal complex $Mn_2(CO)_{10}$: a comparative study, *Acta Cryst. B*, 2003, **59**, 234-247.
27. U. Flierler and D. Stalke, in *Electron Density and Chemical Bonding I: Experimental Charge Density Studies*, ed. D. Stalke, Springer Berlin Heidelberg, Berlin, Heidelberg, 2012, pp. 1-20.
28. R. F. W. Bader, *Atoms in Molecules: A Quantum Theory*, Oxford University Press, 1990.
29. C. Lecomte, M. Souhassou and S. Pillet, Topology of experimental charge density: a tool for understanding atomic interactions, *J. Mo. St.*, 2003, **647**, 53-64.
30. A. B. Vouffack, A. B. Dippenaar, C. Esterhuysen, D. A. Haynes, M. Souhassou, C. Lecomte and N. Claiser, Experimental Charge Density Analysis of p-$O_2NC_6F_4CNSSN^{\bullet}$, a Dithiadiazolyl Molecular Radical, *Cryst. Growth Des.*, 2024, **24**, 8736-8747.

31. B. Gillon, The classical flipping ratio technique applied to non classical magnetic materials : Molecule-based and Photoswitchable magnetic compounds, *J. Phys.*, 2007, 1-30.
32. J. Schweizer, Spin densities in magnetic molecular compounds, *Physica B*, 1997, **234**, 772-779.
33. A. Zheludev, A. Grand, E. Ressouche, J. Schweizer, B. G. Morin, J. A. Epstein, D. A. Dixon and J. S. Miller, The Spin-Density Distribution in the Tetracyanoethylene Radical-Anion, TCNE (Center-Dot-), by Single-Crystal Polarized Neutron-Diffraction, *Angew. Chem. Int. Ed.*, 1994, **33**, 1397-1399.
34. B. Gillon, C. Mathoniere, E. Ruiz, S. Alvarez, A. Cousson, T. M. Rajendiran and O. Kahn, Spin densities in a ferromagnetic bimetallic chain compound: Polarized neutron diffraction and DFT calculations, *J. Am. Chem. Soc.*, 2002, **124**, 14433-14441.
35. C. Aronica, Y. Chumakov, E. Jeanneau, D. Luneau, P. Neugebauer, A. L. Barra, B. Gillon, A. Goujon, A. Cousson, J. Tercero and E. Ruiz, Structure, Magnetic Properties, Polarized Neutron Diffraction, and Theoretical Study of a Copper(II) Cubane, *Chem. Eur. J.*, 2008, **14**, 9540-9548.
36. J. A. Rodriguez-Velamazan, J. S. Costa, J. K. Tang, P. Gamez, J. Campo and J. Luzon, Internal magnetic structure of a Mn3 cluster determined by polarised neutron diffraction, *Acta Cryst. A*, 2008, **64**, C571-C571.
37. Y. Kousaka, T. Koyama, K. Ohishi, K. Kakurai, V. Hutanu, H. Ohsumi, T. Arima, A. Tokuda, M. Suzuki, N. Kawamura, A. Nakao, T. Hanashima, J. Suzuki, J. Campo, Y. Miyamoto, A. Sera, K. Inoue and J. Akimitsu, Monochiral helimagnetism in homochiral crystals of $CsCuCl_3$, *Phys. Rev. Mater.*, 2017, **1**.
38. O. Kahn, Magnetic anisotropy in molecule-based magnets, *Phil. Trans. R. Soc. A*, 1999, **357**, 3005-3023.
39. A. Cornia, D. Gatteschi and R. Sessoli, New experimental techniques for magnetic anisotropy in molecular materials, *Coord. Chem. Rev.*, 2001, **219**, 573-604.
40. A. Gukasov and P. J. Brown, Determination of atomic site susceptibility tensors from polarized neutron diffraction data, *J. Phys. Condens. Matter*, 2002, **14**, 8831-8839.
41. F. Guegan, J. Jung, B. Le Guennic, F. Riobe, O. Maury, B. Gillon, J. F. Jacquot, Y. Guyot, C. Morell and D. Luneau, Evidencing under-barrier phenomena in a Yb(III) SMM: a joint luminescence/neutron diffraction/SQUID study, *Inorg. Chem. Front.*, 2019, **6**, 3152-3157.
42. O. Iasco, Y. Chumakov, F. Guegan, B. Gillon, M. Lenertz, A. Bataille, J. F. Jacquot and D. Luneau, Mapping the Magnetic Anisotropy inside a Ni-4 Cubane Spin Cluster Using Polarized Neutron Diffraction, *Magnetochemistry*, 2017, **3**.
43. K. Ridier, B. Gillon, A. Gukasov, G. Chaboussant, A. Cousson, D. Luneau, A. Borta, J. F. Jacquot, R. Checa, Y. Chiba, H. Sakiyama and M. Mikuriya, Polarized Neutron Diffraction as a Tool for Mapping Molecular Magnetic Anisotropy: Local Susceptibility Tensors in Co-II Complexes, *Chem. Eur. J.*, 2016, **22**, 724-735.
44. D. Luneau and B. Gillon, Polarized Neutron Diffraction: An Excellent Tool to Evidence the Magnetic Anisotropy-Structural Relationships in Molecules, *Magnetochemistry*, 2021, **7**.
45. E. A. Klahn, C. Gao, B. Gillon, A. Gukasov, X. Fabreges, R. O. Piltz, S. D. Jiang and J. Overgaard, Mapping the Magnetic Anisotropy at the Atomic Scale in Dysprosium Single-Molecule Magnets, *Chem. Eur. J.*, 2018, **24**, 16576-16581.

46. K. Ridier, A. Mondal, C. Boilleau, O. Cador, B. Gillon, G. Chaboussant, B. Le Guennic, K. Costuas and R. Lescouezec, Polarized Neutron Diffraction to Probe Local Magnetic Anisotropy of a Low-Spin Fe(III) Complex, *Angew. Chem. Int. Ed.*, 2016, **55**, 3963-3967.
47. T. Kimura, T. Sakurai, M. Shima, T. Togano, M. Mukaida and T. Nomura, Structure of Tetra-μ-Formatodiruthenium Bromide, *Bull. Chem. Soc. Jpn*, 1982, **55**, 3927-3928.
48. M. C. Barral, R. Gonzalez-Prieto, S. Herrero, R. Jimenez-Aparicio, J. L. Priego, M. R. Torres and F. A. Urbanos, Anionic dihalotetraacetatodiruthenium(II,III) compounds, *Polyhedron*, 2005, **24**, 239-247.
49. M. C. Barral, R. Gonzalez-Prieto, R. Jimenez-Aparicio, J. L. Priego, E. C. Royer, M. R. Torres and F. A. Urbanos, Tetra(3-methoxypropionato)diruthenium(II,III) Units: Supramolecular Organization in the Complex $[Ru_2(\mu\text{-}O_2CCH_2CH_2OMe)_4(H_2O)_2]BF_4$, *ZAAC*, 2005, **631**, 2075-2080.
50. M. C. Barral, R. Gonzalez-Prieto, R. Jimenez-Aparicio, J. L. Priego, M. R. Torres and F. A. Urbanos, Synthesis, properties, and structural characterization of bromo- and iodotetracarboxylatodiruthenium(II,III) compounds, *Eur. J. Inorg. Chem.*, 2004, 4491-4501.
51. D. Olea, R. Gonzalez-Prieto, J. L. Priego, M. C. Barral, P. J. de Pablo, M. R. Torres, J. Gomez-Herrero, R. Jimenez-Aparicio and F. Zamora, MMX polymer chains on surfaces, *Chem. Commun.*, 2007, 1591-1593.
52. L. C. Wu, C. W. Hsu, Y. C. Chuang, G. H. Lee, Y. C. Tsai and Y. Wang, Bond Characterization on a Cr-Cr Quintuple Bond: A Combined Experimental and Theoretical Study, *J. Phys. Chem. A*, 2011, **115**, 12602-12615.
53. K. Tahara, T. Morino, Y. Morimoto, Y. Nakamura, K. Sugimoto, Y. Ozawa and M. Abe, Synthetic, Electrochemical, DFT, and Synchrotron X-ray Charge-Density Studies on Oxo-centered Triruthenium Clusters Supported by Electron-Withdrawing Carboxylates, *Inorg. Chem.*, 2024, **63**, 19087-19097.
54. L. C. Wu, T. C. Weng, I. J. Hsu, Y. H. Liu, G. H. Lee, L. Jyh-Fu and Y. Wang, Chemical Bond Characterization of a Mixed-Valence Tri-Cobalt Complex, $Co_3(\mu\text{-admtrz})4(\mu\text{-}OH)_2(CN)_6{\cdot}2H_2O$, *Inorg. Chem.*, 2013, **52**, 11023-11033.
55. R. D. Poulsen, J. Overgaard, A. Schulman, C. Ostergaard, C. A. Murillo, M. A. Spackman and B. B. Iversen, Effects of Weak Intermolecular Interactions on the Molecular Isomerism of Tricobalt Metal Chains, *J. Am. Chem. Soc.*, 2009, **131**, 7580-7591.
56. C. R. Lee, C. C. Wang, K. C. Chen, G. H. Lee and Y. Wang, Bond characterization of metal squarate complexes $M^{II}(C_4O_4)(H_2O)_4$; M = Fe, Co, Ni, Zn, *J. Phys. Chem. A*, 1999, **103**, 156-165.
57. I. Stepanenko, P. Mizetskyi, E. Orlowska, L. Bucinsky, M. Zalibera, B. Vénosová, M. Clémancey, G. Blondin, P. Rapta, G. Novitchi, W. Schrader, D. Schaniel, Y. S. Chen, M. Lutz, J. Kozísek, J. Telser and V. B. Arion, The Ruthenium Nitrosyl Moiety in Clusters: Trinuclear Linear μ-Hydroxido Magnesium(II)-Diruthenium(II), μ3-Oxido Trinuclear Diiron(III)-Ruthenium(II), and Tetranuclear μ4-Oxido Trigallium(III)-Ruthenium(II) Complexes, *Inorg. Chem.*, 2022, **61**, 950-967.
58. C. Lepetit, P. Fau, K. Fajerwerg, M. L. Kahn and B. Silvi, Topological analysis of the metal-metal bond: A tutorial review, *Coord. Chem. Rev.*, 2017, **345**, 150-181.

View Article Online
DOI: 10.1039/D6DT00342G

59. J. F. Van der Maelen and J. A. Cabeza, A topological analysis of the bonding in $M_2(CO)_{10}$ and $M_3(\mu\text{-}H)_3(CO)_{12}$ complexes (M = Mn, Tc, Re), *Theor. Chem. Acc.*, 2016, **135**.
60. C. Gatti and D. Lasi, Source function description of metal-metal bonding in d-block organometallic compounds, *Faraday Discuss.*, 2007, **135**, 55-78.
61. L. J. Farrugia and P. Macchi, in *Electron Density and Chemical Bonding I: Experimental Charge Density Studies*, ed. D. Stalke, 2012, vol. 146, pp. 127-158.
62. A. P. Ginsberg and M. E. Lines, Magnetic Exchange in Transition Metal Complexes. VIII. Molecular Field Theory of Intercluster Interactions in Transition Metal Cluster Complexes, *Inorg. chem.*, 1972, **11**, 2289-2290.
63. R. J. Papoular and B. Gillon, Maximum-Entropy Reconstruction of Spin-Density Maps in Crystals from Polarized Neutron-Diffraction Data, *Europhys. Lett.*, 1990, **13**, 429-434.
64. P. Schleger, A. PuigMolina, E. Ressouche, O. Rutty and J. Schweizer, A general maximum-entropy method for model-free reconstructions of magnetization densities from polarized neutron diffraction data, *Acta Cryst. A*, 1997, **53**, 426-435.
65. K. D. Demadis, C. M. Hartshorn and T. J. Meyer, The Localized-to-Delocalized Transition in Mixed-Valence Chemistry, *Chem. rev.*, 2001, **101**, 2655-2686.
66. B. O. Roos, A. C. Borin and L. Gagliardi, Reaching the maximum multiplicity of the covalent chemical bond, *Angew. Chem. Int. Ed.*, 2007, **46**, 1469-1472.
67. N. Fritsch, C. R. Wick, T. Waidmann, P. O. Dral, J. Tucher, F. W. Heinemann, T. E. Shubina, T. Clark and N. Burzlaff, Multiply Bonded Metal(II) Acetate (Rhodium, Ruthenium, and Molybdenum) Complexes with the trans-1,2-Bis(N-methylimidazol-2-yl)ethylene Ligand, *Inorg. Chem.*, 2014, **53**, 12305-12314.
68. A. D. Becke, Density-functional thermochemistry. III. The role of exact exchange, *J. Chem. Phys.*, 1993, **98**, 5648-5652.
69. C. T. Lee, W. T. Yang and R. G. Parr, Development of the Colle-Salvetti Correlation-Energy Formula into a Functional of the Electron-Density, *Phys. Rev. B*, 1988, **37**, 785-789.
70. P. J. Stephens, F. J. Devlin, C. F. Chabalowski and M. J. Frisch, Ab-Initio Calculation of Vibrational Absorption and Circular-Dichroism Spectra Using Density-Functional Force-Fields, *J. Phys. Chem.*, 1994, **98**, 11623-11627.
71. R. Maurice, R. Bastardis, C. de Graaf, N. Suaud, T. Mallah and N. Guihéry, Universal Theoretical Approach to Extract Anisotropic Spin Hamiltonians, *J. Chem. Theory Comput.*, 2009, **5**, 2977-2984.
72. C. Angeli, R. Cimiraglia, S. Evangelisti, T. Leininger and J. P. Malrieu, Introduction of n-electron valence states for multireference perturbation theory, *J. Chem. Phys.*, 2001, **114**, 10252-10264.
73. C. Angeli, R. Cimiraglia and J. P. Malrieu, N-electron valence state perturbation theory:: a fast implementation of the strongly contracted variant, *Chem. Phys. Lett.*, 2001, **350**, 297-305.
74. C. G. Pech, P. A. B. Haase, N. Galland, A. Borschevsky and R. Maurice, Relevance of effective bond orders in heterodiatomic molecules and role of the spin-orbit coupling in the AtX (X = At – F) series, *Phys. Rev. A*, 2019, **100**.
75. Agilent, CrysAlis PRO.*Journal*, 2014.
76. F. H. Allen, Systematic Pairwise Comparison of Geometric Parameters Obtained by X-Ray and Neutron-Diffraction, *Acta Cryst. B*, 1986, **42**, 515-522.

77. F. H. Allen and I. J. Bruno, Bond lengths in organic and metal-organic compounds revisited: X-H bond lengths from neutron diffraction data, *Acta Cryst. B*, 2010, **66**, 380-386.
78. R. H. Blessing, Data Reduction and Error Analysis for Accurate Single Crystal Diffraction Intensities, *Crystallogr. Rev.*, 1987, **1**, 3-58.
79. L. J. Bourhis, O. V. Dolomanov, R. J. Gildea, J. A. K. Howard and H. Puschmann, The Anatomy of a Comprehensive Constrained, Restrained, Refinement Program for the Modern Computing Environment - Olex2 Disected, *Acta Cryst. A*, 2015, **A71**, 59-71.
80. E. Clementi and D. L. Raimondi, Atomic Screening Constants from Scf Functions, *J. Chem. Phys.*, 1963, **38**, 2686-&.
81. O. V. Dolomanov, L. J. Bourhis, R. J. Gildea, J. A. K. Howard and H. Puschmann, OLEX2: a complete structure solution, refinement and analysis program, *J. Appl. Crystallogr.*, 2009, **42**, 339-341.
82. M. Douglas and N. M. Kroll, Quantum Electrodynamical Corrections to Fine-Structure of Helium, *Annals of Physics*, 1974, **82**, 89-155.
83. B. Guillot, L. Viry, R. Guillot, C. Lecomte and C. Jelsch, Refinement of proteins at subatomic resolution with MOPRO, *J. Appl. Crystallogr.*, 2001, **34**, 214-223.
84. M. Handa, H. Yairi, Y. Koyama, R. Mitsuhashi and M. Mikuriya, Polynuclear Chain Compound of Tetrakis(mu-n-butyrato-O,O ')diruthenium Bromide, *X-ray Struct. Anal. Online*, 2022, **38**, 21-23.
85. G. Jansen and B. A. Hess, Revision of the Douglas-Kroll Transformation, *Phys. Rev. A*, 1989, **39**, 6016-6017.
86. F. Neese, Efficient and accurate approximations to the molecular spin-orbit coupling operator and their use in molecular g-tensor calculations -: art. no. 034107, *J. Chem. Phys.*, 2005, **122**.
87. D. A. Pantazis, X. Y. Chen, C. R. Landis and F. Neese, All-electron scalar relativistic basis sets for third-row transition metal atoms, *J. Chem. Theory Comput.*, 2008, **4**, 908-919.
88. B. O. Roos, P. R. Taylor and P. E. M. Siegbahn, Complete Active Space SCF Method (CASSCF) Using a Density-Matrix Formulated Super-CI Approach, *Chem. Phys.*, 1980, **48**, 157-173.
89. G. M. Sheldrick, SHELXT - Integrated space-group and crystal-structure determination, *Acta Cryst. A*, 2015, **71**, 3-8.
90. G. M. Sheldrick, Crystal structure refinement with SHELXL, *Acta Cryst. C*, 2015, **71**, 3-8.

View Article Online
DOI: 10.1039/D6DT00342G

Data availability

Electronic supplementary information (ESI) available report experimental details on synthesis, characterization and crystal growing of (NBu_4) $[Ru_2^{V}Br_2(O_2CCH_3)_4]$, High-resolution X-Ray diffraction crystal structure, Experimental electron density model, Magnetic measurements, Neutron diffraction, Polarized neutron diffraction, Experimental spin density model and magnetic susceptibility tensors determination, Quantum mechanical calculations complemented by additional Tables and Figures for crystal structures electron density, spin density and magnetism; The crystallographic information files (CIF), containing the X-ray crystallographic data with embedded multipole model and experimental structure factors and non-polarised neutron data has been deposited at The Cambridge Crystallographic Data Centre,12 Union Road, Cambridge CB2 1EZ, UK; fax: +44 1223 336 033. (CCDC deposition number 2516707 and 2519322). The authors have cited additional references within Supporting Information.[23, 42, 66, 71-73, 75-90]